



Time-resolved photoluminescence spectroscopy in GaN-based semiconductors with micron spatial resolution

T. Izumi^{a,*}, Y. Narukawa^a, K. Okamoto^b, Y. Kawakami^a, Sg. Fujita^a, S. Nakamura^c

^aDepartment of Electronic Science and Engineering, Kyoto University, Kyoto 606-8501, Japan

^bVenture Business Laboratory, Kyoto University, Kyoto 606-8501, Japan

^cDepartment of Research and Development, Nichia Chemical Industries Ltd., 491 Oka, Kaminaka, Anan, Tokushima 774-8601, Japan

Abstract

Recombination dynamics in GaN-based layers have been studied by means of photoluminescence spectroscopy having spectral and spatial resolution. It was found that PL lifetime (τ_{PL}) of the epitaxially laterally overgrown GaN (ELO-GaN), which consists of the regions with high (window) and low (wing) threading dislocation density (DD), was dominated by the nonradiative recombination process at room temperature (RT), and that the τ_{PL} measured at wing region (DD = 10^6 cm^{-2}) was 86 ps which is slightly larger than the value (70 ps) at window region (DD = 10^8 cm^{-2}). These indicate that threading dislocations limit hardly the emission efficiency even with these DD-levels, and that the device performance is mainly limited by other types of nonradiative recombination centers. © 2000 Elsevier Science B.V. All rights reserved.

Keywords: Spatial and time-resolved spectroscopy; ELO-GaN; Threading dislocation; Nonradiative process

1. Introduction

Current progress in the fabrication technology of GaN-based semiconductors has led to the realization of incandescent blue and green light-emitting diodes (LEDs). In spite of high threading dislocation density (DD = 10^8 – 10^{10} cm^{-2}) in epilayers grown on sapphire, such LEDs show a substantially high external quantum efficiency (η_{ext}) of about 10%. However, further improvement of the efficiency is desired to extend the application area of LEDs. Mukai et al. [1] reported that the efficiency of blue LED, whose defect density is lowered by the epitaxial lateral overgrowth (ELO) technique, is almost the same as that of conventional LEDs grown directly on sapphire. On the other hand, Sugahara et al. [2] showed by a comparison between transmission electron microscopy (TEM) and cathodoluminescence (CL) mapping that dislocations do act as nonradiative recombination centers (NRC). Moreover, Chichibu et al. reported that

lifetime of photoluminescence (PL) did not almost depend on DD in ELO-GaN by selective-photo-excitation using metal-masking technique [3]. Consequently, it is very important for the improvement of η_{ext} to elucidate a detailed correlation between microscopic structures and macroscopic optical properties. This can be facilitated by the assessment of radiative and nonradiative recombination processes by employing site-selective time-resolved photoluminescence (TRPL) spectroscopy with a spatial resolution of less than a few microns. In this paper, we studied the recombination dynamics in GaN-based layers using the spatial and time-resolved spectroscopy.

2. Experimental procedure

The samples used in this study were of three types, one was (a) ELO-GaN, another was (b) 4 μm -GaN directly grown on sapphire (0 0 1), and the third was (c) bulk GaN (100 μm) grown on ELO-GaN and after the growth the sapphire substrate was polished off. All samples were grown by metalorganic chemical vapor deposition (MOCVD). Their threading dislocation densities were roughly estimated to be (a) 10^6 cm^{-2} in wing region,

* Corresponding author. Tel.: + 81-75-753-5357; fax: + 81-75-753-5898.

E-mail address: t-izumi@fujita.kuee.kyoto-u.ac.jp (T. Izumi)

10^8 cm^{-2} in window region, (b) 10^8 cm^{-2} and (c) 10^6 cm^{-2} , respectively. For cw photoluminescence (PL) measurements, the excitation source was a He–Cd laser (325 nm). PL detection was carried out using a multi-channel analyzer. The light source used for reflection measurement was obtained by passing the Xe-lamp through a 25 cm monochromator. The reflection signals were detected by a Si-photodiode and amplified by a lockin amplifier. Fig. 1 shows the TRPL measurement system with micron spatial resolution. The pulsed excitation was provided by third harmonic generated beam of a mode-locked $\text{Al}_2\text{O}_3 : \text{Ti}$ laser which was pumped by Ar^+ -laser. The wavelength, the pulse width and the repetition rate were 266 nm, 1.5 ps and 80 MHz, respectively. The beam was focused down to the size with diameter of a few microns using air-gapped object lens. Fluorescent image can be observed by optical microscope in conjunction with CCD camera, and be detected through UV-optical fiber in order to measure the TRPL using a synchroscan streak camera in conjunction with a 25 cm monochromator.

3. Results and discussion

Fig. 2(i) shows reflection spectrum from sample (a) and PL spectra of the three samples at 20 K. The reflection spectrum shows A-free exciton (E_{XA}) and B-free exciton (E_{XB}) at 3.495 and 3.503 eV, respectively. Accordingly, the PL peak of sample (a) located at 3.494 eV and the main peak located at 3.487 eV are attributed to the E_{XA} and the neutral donor-bound exciton [(D^0, X)], respectively. Each PL spectrum has two major peaks, indicating that the main peak originates from (D^0, X) , and another peak from E_{XA} . The E_{XA} emission of sample (a) located at 3.494 eV is the largest energy in the three samples. The dashed line is the energy (3.4780 eV) of E_{XA} emission from stress-free GaN grown homoepitaxially by MOCVD on GaN substrate [4]. Hence, sample (a) undergoes the largest in-plane biaxial compressive strain caused by the difference of thermal coefficient between GaN and sapphire substrate. Fig. 2(ii)

shows PL spectra from sample (a) at various temperatures from 20 K to RT. At low temperature, under 40 K, PL is dominated by (D^0, X) emission, and with increasing temperature, PL comes to be dominated by E_{XA} emission and the PL peak shifts to lower energy in accordance with the temperature dependence of band gap [5]. The PL spectrum at RT is composed of E_{XA} emission associated with LO-phonon replica whose shoulder on high-energy side is contributed from E_{XB} . PL integrated intensity decreased to 1% of the intensity at 20 K with increasing the temperature to RT. This is because nonradiative recombination process dominates the recombination of the photogenerated carriers with increasing temperature. Similar measurement was also done for samples (b) and (c). As a result, a similar tendency was found, indicating that threading dislocations do not affect largely nonradiative recombination process.

The dynamical behaviors of radiative and non-radiative recombination process were assessed by means of TRPL spectroscopy. For sample (a), we employed TRPL with a spatial resolution of a few microns (focused laser beam size in this measurement was $2 \times 3 \mu\text{m}$), which made it possible to measure several τ_{PL} either from wing region ($DD = 10^6 \text{ cm}^{-2}$) or from window region ($DD = 10^8 \text{ cm}^{-2}$) as shown in Fig. 3(i). It should be noted that the transfer process of photogenerated carriers between wing and window regions can be neglected because the diffusion length of GaN is as small as about 50 nm [2]. Fig. 3(ii) shows the decay spectra of PL intensity from the E_{XA} band for each sample at RT. The signal intensity is shifted to each other for ease of comparison. Fig. 3(ii) – (1), (3) and (5) show the decay spectra with large focused laser beam size (100 μm in diameter) from samples (b), (a) and (c), respectively. Only in sample (a), the luminescence decay spectra of the E_{XA} from window region and wing region with small focused laser beam size ($2 \times 3 \mu\text{m}$) are also shown in Fig. 3(ii) – (2) and (4), respectively. Hence, DD decreases with increasing the index number from (1) to (5). All decay spectra [$I(t)$] are well fitted with multi-exponential curve as shown below.

$$I(t) = A_1 \exp(-t/\tau_1) + A_2 \exp(-t/\tau_2). \quad (1)$$

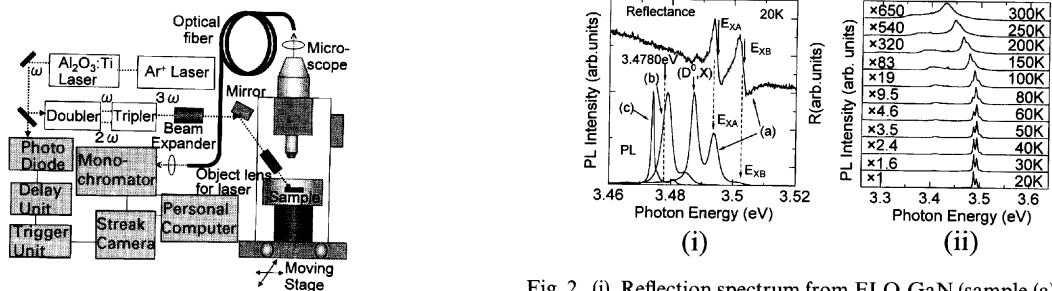


Fig. 1. TRPL measurement system in conjunction with UV-optical microscope.

Fig. 2. (i) Reflection spectrum from ELO-GaN (sample (a)) and PL spectra from ELO-GaN (sample (a)), 4 μm -GaN (sample (b)) and bulk GaN (sample (c)) at 20 K. (ii) PL spectra of ELO-GaN (sample (a)) taken at various temperatures from 20 K to RT.

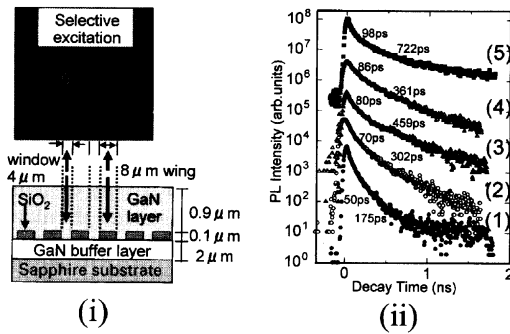


Fig. 3. (i) The image of ELO-GaN observed by optical microscope. And cross figure of ELO-GaN. The window region is selectively excited by focused laser beam. (ii) Decay spectra of PL intensity of E_{XA} band at RT taken by macroscopic photoexcitation (100 μm in diameter) from (1) 4 μm -GaN (sample (b)), (3) ELO-GaN (sample (a)) and (5) bulk GaN (sample (c)), and by microscopic photoexcitation ($2 \times 3 \mu\text{m}$) from ELO-GaN (sample (a)) (2) at window region ($\text{DD} = 10^8 \text{ cm}^{-2}$) and (4) at wing region ($\text{DD} = 10^6 \text{ cm}^{-2}$). The photoexcitation energy density was $3.4 \mu\text{J}/\text{cm}^2$ for whole measurements.

This result cannot be interpreted only with two-competing processes, namely, (P1) radiative recombination and (P2) nonradiative one where excitons and/or carriers are captured to the defects caused by diffusion process. Two feasible models can be applied in order to account for this behavior, where (i) photoexcited area contains two regions having different recombination times, and (ii) radiative recombination is partly contributed from bimolecular process. If the latter is the case, the first component (τ_1) decreases and the A_1/A_2 value increases with increasing photoexcitation energy density (I_{ex}). However, it was found that both τ_1 and the second component (τ_2) increased, while A_1/A_2 stayed at almost constant if I_{ex} value is raised [6]. These results indicate that model (i) is proper in this case, and that both τ_1 and τ_2 are limited by the channel of non-radiative recombination. In fact, temperature dependence of PL intensity [Fig. 2(ii)] also supports that the recombination of excitons is mostly due to nonradiative process at RT. The inserted numbers in Fig. 3(ii) are estimated values of τ_1 and τ_2 for each sample. Hereafter, we discuss how τ_1 value changes with samples because the fast process limits the PL decay process compared with the slow one. It was found that $\tau_1(\tau_{\text{PL}})$ values under macroscopic photoexcitation were 50, 80 and 98 ps in samples (b), (a) and (c), respectively, indicating that the smaller DD makes τ_{PL} somewhat longer. Furthermore, it was found that τ_{PL} measured at wing region ($\text{DD} = 10^6 \text{ cm}^{-2}$) excited microscopically was 86 ps which is slightly larger than the value monitored at window region (70 ps) whose DD is two orders of magnitude larger than that in the wing region, indicating the higher density of NRC in the window region. In each sample at RT, recombination process

of photogenerated carriers is mainly dominated by non-radiative recombination channel and τ_{PL} is almost equal to the lifetime of nonradiative recombination ($\tau_{\text{non-rad}}$). On the other hand, $\tau_{\text{non-rad}}$ is given by the equation

$$1/\tau_{\text{non-rad}} = N_t v_{\text{th}} \sigma, \quad (2)$$

where N_t , v_{th} and σ represent the density of NRC, the thermal velocity of carriers and the cross capture area of carriers, respectively. If the N_t arises only from DD, a two orders of magnitude increase in DD should make $\tau_{\text{non-rad}}$ decrease by two orders of magnitude. However, τ_{PL} did not differ so largely between the smallest- and the largest-DD samples. This indicates that threading dislocations hardly limit the emission efficiency at these DD-levels as can be understood as a result of small diffusion length of GaN-based semiconductors [1,2]. Consequently, device performance is probably affected mainly by other types of NRC whose origin is probably point-defect-like centers.

4. Conclusion

We studied the recombination dynamics in GaN-based layers using the spatial and time-resolved spectroscopy. The beam was focused down to the size with diameter of a few microns using air-gapped object lens. It was found that τ_{PL} was limited by the nonradiative recombination channel, and that τ_{PL} values at $\text{DD} = 10^6$, and 10^8 cm^{-2} were 86 and 70 ps, respectively, indicating the importance of other types of NRC limiting device performance at RT. The origin can be ascribed to point-defect-like centers because they cannot be detected by the observation by transmission electron microscopy.

Acknowledgements

This work was partly supported by a Grant-in-Aid for Scientific Research from the Ministry of Education, Science, Sports and Culture, Japan, Tateishi Science and Technology Foundation, Tokuyama Science and Technology Foundation and Hoso Bunka Foundation.

References

- [1] T. Mukai, K. Takekawa, S. Nakamura, Jpn. J. Appl. Phys. 37 (1998) L839.
- [2] T. Sugahara et al., Jpn. J. Appl. Phys. 37 (1998) L398.
- [3] S. Chichibu et al., Appl. Phys. Lett. 74 (1999) 1460.
- [4] Porowski, Solid State Commun. 97 (11) (1996) 919.
- [5] S. Chichibu, T. Azuhata, T. Sota, S. Nakamura, J. Appl. Phys. 79 (1996) 2784.
- [6] T. Izumi, Y. Narukawa, K. Okamoto, Sz. Fujita, Sg. Fujita, S. Nakamura, unpublished data.